# Data Science Guided Experiments Identify Conjugated Polymer Solution Concentration as a Key Parameter in Device Performance

Rahul Venkatesh,[‡] Yulong Zheng,[†] Campbell Vierson,[†] Aaron Liu[‡] , Carlos Silva,[†,§,||] Martha Grover,[‡,*] and Elsa Reichmanis[¶,*]

[‡]*School of Chemical and Biomolecular Engineering, Georgia Institute of Technology, 311 Ferst Drive NW, Atlanta GA 30332, United States*

[†]*School of Chemistry and Biochemistry, Georgia Institute of Technology, 901 Atlantic Drive, Atlanta GA 30332, United States*

[§]*School of Physics, Georgia Institute of Technology, 837 State Street, Atlanta GA 30332,United States*

[||]*School of Materials Science and Engineering, Georgia Institute of Technology, 771 Ferst Drive NW, Atlanta GA 30332, United States*

[¶]*Department of Chemical & Biomolecular Engineering, Lehigh University, 111 Research Drive W, Bethlehem PA 18015, United States*

E-mail: elr420@lehigh.edu; martha.grover@chbe.gatech.edu

**Abstract**

Curating and analyzing centralized data repositories is a valuable approach in resolving the issue of reproducibility, gaining new insights and guiding future experiments, especially in the field of nano-materials research. In this work, a dataset containing processing information and mobility values of 115 DPP-DTT-based Organic Field Effect Transistors (OFET) was constructed from 15 publications. A customized classification algorithm was applied to the dataset to help identify a reduced design region for polymer solution concentration that would be more likely to result in improved hole mobility. Experiments performed to confirm the insights from the data curation exercise revealed a strong influence of solution concentration on the polymer chain excitonic interactions and electronic performance. Devices fabricated at the critical chain overlap concentration of 5 g/L in chlorobenzene resulted in improved hole mobility, and were in good agreement with the insights provided by the classification algorithm.

Semiconducting polymeric materials have demonstrated great potential in the production of light-weight, low-cost devices such as organic photovoltaics (OPVs),[1] OFETs,[2] organic light emitting diodes (OLEDs),[3] and biomedical sensors.[4] The application of these materials in electronic devices relies on their ability to efficiently transport charges within the pi-conjugated network. Many polymer semiconductors are believed to be comprised of ordered and disordered regions,[5] whereby charges move between ordered structures by travelling along bridging tie chains. The charge transport mechanism has been extensively studied in conjugated semi-crystalline homopolymers such as poly[3-hexylthiophene-2,5-diyl] (P3HT) and poly[2,5-bis(3-tetradecylthiophen-2-yl)thieno[3,2-b]thiophene] (PBTTT), which possess a significant volume fraction of extended crystalline regions and typically exhibit mobilities in the range of 0.05 – 1 $cm^2/Vs$.[6] Suggested design guidelines to achieve high mobility in homopolymers include the need for a crystalline lamellar structure with long-range order and extended $\pi$-$\pi$ overlap oriented parallel to the substrate.[7-9] Previous work on these materials indicates that apart from the polymer intrinsic properties, solution processing and thin-film deposition conditions also impact the morphology, microstructure, and electrical performance of the final thin-film device.[10-16] There is thus a vast and complex design space that is inefficient to explore via an Edisonian approach.[17] Additionally, the lack of standardized reporting of processing conditions hinders experimental reproducibility and consequently hampers research progress.[18]

Curating accurate and interpretable process-property datasets helps promote reproducibility and transparency in several fields of research, and enables development of experimental design algorithms for process optimization.[19, 20] Analysis of these datasets can confirm existing hypotheses and guide future experimental studies. In a previous study, Persson *et al.*[19] compiled a database containing process-property information of over 200 P3HT-based OFET devices curated from 19 publications. Despite the conjugated polymer remaining consistent across all devices, reported values for the charge carrier mobility varied by over six orders of magnitude ($10^{-6}$ to $10^{-1}$ $cm^2$.Vs), indicating the strong influence of intrinsic material properties and processing conditions on charge carrier mobility. Basic analysis on the dataset confirmed well-known trends such as the effect of polymer molecular weight, transistor channel length, and deposition method on hole mobility. Subsequently, McBride *et al*[20]. applied a customized classification approach on the continuous design variables and identified the necessary processing parameters required to confine the high-performing points to a reduced design region (RDR), which can be used to guide future experiments.

More recently discovered push-pull copolymers, commonly referred to as donor-acceptor (D-A) polymers, with a polymer backbone consisting of alternating electron-deficient (acceptor) and electron-rich (donor) units, have exhibited far higher mobilities compared to the semicrystalline homopolymers,[15, 21] even though their microstructure is typically more disordered with smaller crystalline aggregates.[6] The high mobility observed in D-A polymers has been attributed to the rigid, planar backbone conformation with minimal steric hinderance between the donor and acceptor units. Unlike homopolymers, significant knowledge gaps exist in the process-structure-property relationships of D-A copolymers creating opportunities to optimize OFET performance still further. In this work, we compile a process-property dataset derived from 115 published OFET devices fabricated using the commercially available D-A polymer, poly[2,5-(2-octyldodecyl)-3,6-diketopyrrolopyrrole-alt-5,5-(2,5-di(thien-2-yl)thieno-[3,2-b]-thiophene)]

(DPP-DTT). The classification approach developed by McBride *et al*. was extended to this system to gain new insights and guide experimental studies. Interestingly, the algorithm identified polymer solution concentration as a key factor in device performance and recommended a reduced design range for this processing variable expected to result in high performing devices. Whereby to the best of our knowledge, polymer concentration has not been identified as a key metric linked to macroscale device performance. Experimental results correlated very well with the insights gained from the data curation and analysis exercise. Viscosity measurements of the solutions at increasing concentrations revealed a two-regime behavior that is likely attributed to the overlap of polymer chains in solution state. Additionally, UV-vis absorption spectra of the solid thin-films suggested a likely decrease in intrachain interactions (J-aggregate behavior) and increase in interchain interactions (H-aggregate behavior) with increasing solution concentration. Lastly, OFETs fabricated from DPP-DTT solutions at the concentration range recommended by the classification algorithm exhibited improved hole-mobility, highlighting the advantage of integrating materials informatics approaches into the existing polymer electronics paradigm.

In this work, a dataset comprising processing information and performance metrics associated with 115 DPP-DTT based OFET devices from 15 publications was curated and analyzed. The list of publications utilized for curating this dataset is provided in the supporting information. The classification algorithm developed by McBride *et al.*[20, 22] was applied to the curated dataset to identify the most impactful processing variables from a list of 21 numerical variables that confine the devices with a "high" field effect transistor (FET) hole mobility ( > 1 $cm^2/V.s$) to a reduced design space The advantage of this algorithm is that it selects the key processing parameters from a long list of variables—thus preventing the need to investigate all the processing variables individually, which can be tedious and time-consuming. The full classification approach is discussed in detail in the Supporting Information (SI) (Figure S1-S3) along with the corresponding code. The best features selected by the algorithm were plotted as a function of the hole mobility to confirm the existing hypothesis, gain new insights and guide future experiments.

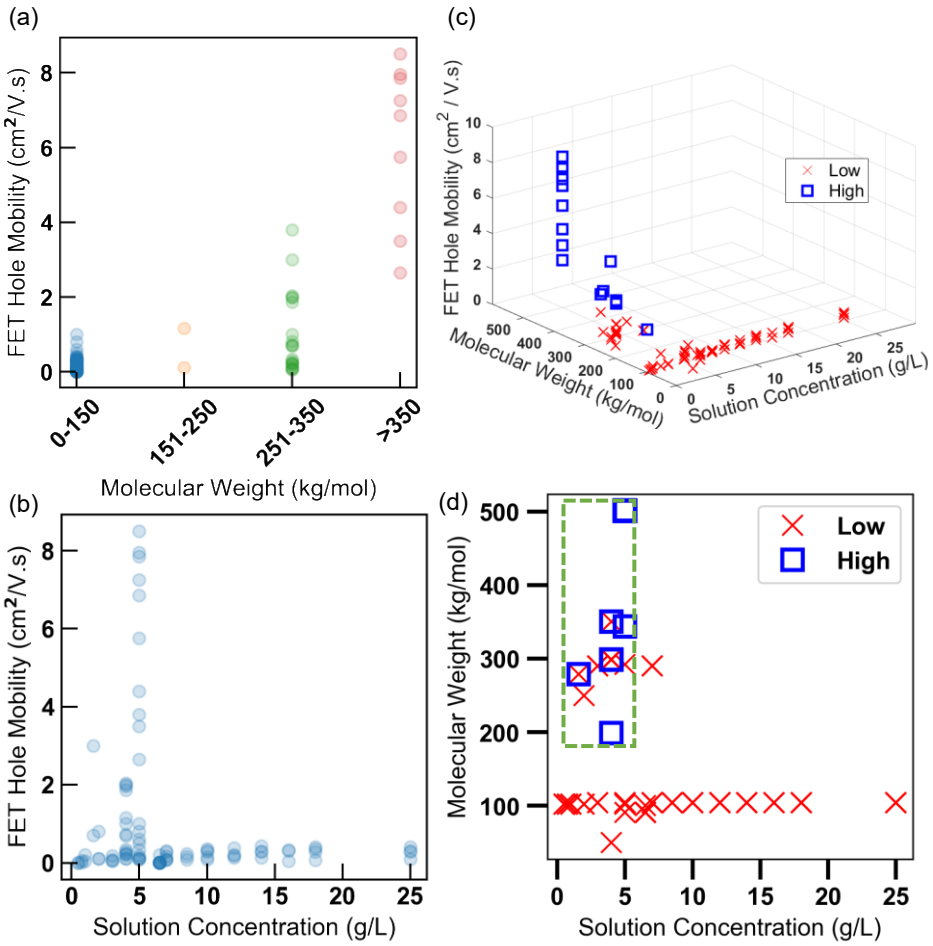


*Figure 1.FET hole mobility versus (a) groups of weight average molecular weight (kg/mol), (b) solution concentration(g/L) and (c) weight average molecular weight (kg/mol) and solution concentration(g/L) as a three-dimensional plot. (d) Two-dimensional reduced design spaces containing all devices with hole mobility values above and below the cutoff of 1 $cm^2$/V.s for easier visualization. Blue squares are "High" data points above the cutoff(> 1 $cm^2$/V.s), red x markers represent "Low" data points below the cutoff(<= 1 $cm^2$/V.s), and the green dashed-lines represents the boundary of the reduced design region in the 2D spaces containing all the "high" points and some "low" points. Figure 1c and d contain a total of 16 "high" points and 76 " low" points, with some of the points overlapping each other.*

The key processing parameters identified by the algorithm based on user-defined specifications (i.e. those that were able to best confine the "high" performing devices to a reduced design space) include weight average molecular weight ($M_w$), number average molecular weight ($M_n$), solution concentration (g/L), polydispersity and dielectric capacitance (nF/$cm^2$) (See Figure S3 in SI). The FET hole mobility increasing as a function of $M_w$, is shown in Figure 1a. This trend agrees with findings from existing studies on conjugated polymers whereby higher polymer $M_w$ typically results in longer polymer chains that can connect ordered crystalline domains and offer enhanced charge transport performance.[15, 21] Perhaps more interesting and as can be discerned from Figure 1b, higher mobilities were obtained for devices prepared from solutions having a concentration between 4 and 5 g/L. 10 out of the 16 "high" performing devices used a concentration of 5 g/L with chlorobenzene (CB) as the solvent. Additional detail comparing the processing conditions for the "high" performing devices is provided in the supporting information. Conceivably, the majority of studies selected a solution concentration in this range to stay consistent with literature reports. The exact influence of this processing parameter on charge carrier mobility of push-pull polymers has not been widely investigated and provides an

opportunity for further studies. Analysis of the other three key processing parameters can be obtained from the code available in the supporting information. This insight highlights the advantage of the data curation exercise to uncover knowledge gaps. Finally, subsets of the best features can be analyzed simultaneously, and a RDR bounded by high-performing points can be evaluated to guide future experiments. Results from Figure 1c indicate that choosing a value of $M_w$ between 200-500 kg/mol and solution concentration between 2-5 g/L would be more likely to result in a high-performing OFET device.

As recommended by the RDR algorithm, DPP-DTT (Figure 2a), with a $M_w$ of 290 kg/mol, in chlorobenzene was used as an initial system of interest. Solution concentrations ranging from 1–8 g/L were prepared from a stock of 10 g/L. Note, the solution-state of conjugated polymers is typically neglected and needs to be studied to establish clear relationships between solution-state structures, solid-state morphology and charge transport properties.[23] Viscosity measurements of the solutions at different concentrations were conducted to explore the influence of solution concentration on the behavior of polymer chains in the solution state.

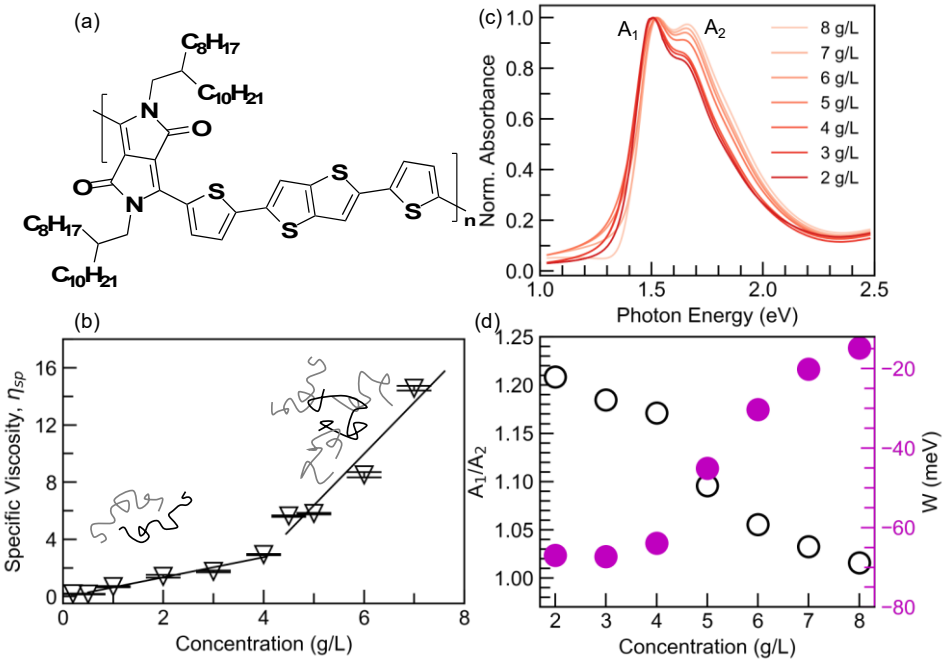


*Figure 2. (a) Schematic of molecular structure of DPP-DTT. (b) Viscosity measurement of DPP-DTT dissolved in chlorobenzene solutions at 56 °C. The error bars represent the standard deviation of the specific viscosity (open triangles). The schematic illustrates the extended, isolated polymer chains in dilute solutions and kinky, intertwined polymer chains in semi-dilute solutions.(c) Linear absorption spectra of DPP-DTT thin films prepared from solution concentrations ranging from 2 to 8 g/L. (d) $A_1/A_2$ ratio (open circle) and exciton bandwidth (filled circle) acquired from Franck Condon simulations as a function of concentration.*

We discerned an expected increase in the specific viscosity with increasing solution concentration as seen in Figure 2b. An interesting observation was the presence of a two-regime behavior, with the cross-over occurring ~ 5 g/L, which can be attributed to the critical chain overlap point C*.[24, 25] This behavior suggests that the polymer chains or aggregates are more extended and isolated at dilute concentrations (< C* g/L), then start to overlap when the concentration surpasses C* and finally become entangled as displayed in Figure 2b. The solution-state absorption spectra of 2 and 8 g/L polymer solutions as shown in Figure S14 in

SI, display a more dominant J-like character compared to the corresponding solid-state films, indicating that polymer chains in solution are more isolated than solidified thin films even in semi-dilute regime.

To transfer the chain overlap effect from the solution state to the solid film state, a series of wire-bar coated films were prepared from polymer-CB solutions ranging in concentration from 2 to 8 g/L, with the substrate and solution temperatures being maintained at 56 °C. To probe the influence of solution concentration on the polymer excitonic chain interactions, the photophysical features of the solid thin films were examined using steady-state UV-vis absorption spectroscopy as presented in Figure 2c. Here, we focus on the low energy band where localized excitation on the DPP unit is dominant.[26] Analogous to P3HT, the coupling between the electronic excitation and aromatic ring stretching mode could still lead to pronounced vibronic progressions.[27] The ratio of the vibronic progressions of $A_1$ and $A_2$ peaks are provided in Figure 2d and is observed to be consistently higher than 1, which might be due to the J-type nature of strong intrachain charge-transfer character as investigated recently by Qarai *et al.*[27] A decreasing trend for the $A_1/A_2$ with increasing solution concentration indicates that films coated from semi-dilute solutions (> C*) may adopt more H-aggregate configurations than films prepared from dilute solutions (< C*). Additionally, the modified Franck Condon (FC) analysis (assuming a Huang-Rhys factor of 1) was performed within the exciton resonance region from 1.4 to 1.8 eV to extract the *effective* exciton bandwidth (W), which quantifies the effective interchain coupling constant.[28] The complete set of FC fits for the absorption spectra of each concentration along with the parameters obtained for the same is presented in Figure S4 in the SI. The magnitude of W decreases with increasing concentration, corresponding to a smaller coupling constant, indicating an increasing H-type interchain interaction (Figure 2d).[29, 30] Moreover, with increasing H-type coupling, the $A_1$ peaks are observed to blue-shift slightly which is consistent with the H-aggregate model.[28, 31] It is worth pointing out, the different electronegativity between donor and acceptor units also modifies the Kasha model which assumes no wavefunction overlap.[29, 32] Nevertheless, the intrachain charge-transfer character/Frenkel exciton mixing as well as interchain Coulombic interactions would give rise to similar Kasha spectral features[27, 29] and the modified FC progression takes into account the contribution from excitonic dispersion in the weak coupling limit. The exciton bandwidth and coupling constant could be understood as an *effective* term. Moreover, the spectral features and the magnitude of exciton bandwidths reproduced by the HJ aggregate model are mostly consistent with situations seen in semicrystalline P3HT within the weakly-coupled limit.[28, 33] Thus, we suggest that as both the $A_1/A_2$ and W trends exhibit two regime behavior, analogous to the viscosity results, the chain entanglements inherent in polymer solutions may be preserved in the solidified films. Transient absorption measurements are expected to provide further insight regarding the impact of chain entanglement on the photoinduced absorption line shape. The surface microstructure of thin films at different concentrations were also investigated using atomic force microscopy (AFM) and cross-polarized optical microscopy (CPOM), and the images are presented in Figure S9 and S10 respectively in the SI.

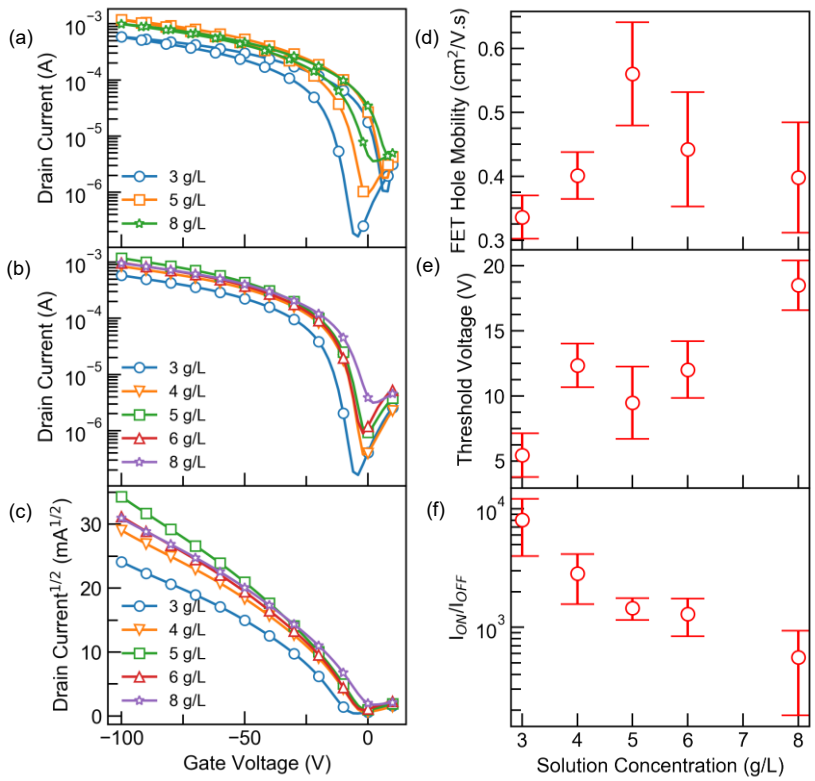


*Figure 3.* **Transfer *Characteristics ($V_{DS}$ = -80V) and OFET parameters of interest for DPP-DTT thin films as a function of solution concentration.*** *(a) Forward and backward sweep $I_D - V_G$ curves at concentrations of 3, 5 and 8 g/L exhibiting hysteresis. (b) and (c) Backward sweep transfer characteristics ($V_{DS}$ = -80V) as a function of solution concentration. (d) and (e) FET hole mobility and threshold voltage extracted from the backward sweep transfer curve ($I_D^{1/2}$ - $V_G$) as a function of solution concentration. (f) $I_{on}/I_{off}$ obtained from the backward sweep transfer curve ($I_D - V_G$) as a function of solution concentration. The error bars here represent 95% confidence intervals averaged over 8-12 OFET devices.*

The electronic performance of the films at different concentrations was investigated by fabricating OFETs using bottom-gate bottom-contact Si/$SiO_2$ substrates. The respective transfer and output characteristics are shown in Figure 3 and Figure S4, respectively. Rationale for the observed deviation from ideal behavior (hysteresis and different slope regions) is provided in the SI. The hole mobility, threshold voltage and $I_{on}/I_{off}$ as a function of solution concentration extracted from the backward sweep, are presented in Figure 3d, e and f, respectively. Figure 3b indicates a clear increase in hole mobility as the dilute concentrations increase to C* (5 g/L) followed by a decrease in the average mobility. Although, the mobility value at 5 g/L does not cross the threshold (1 cm$^2$/V.s) set during the analysis of the curated OFET dataset, the results in general are in good agreement with the insights from the classification algorithm. It is important to note that device measurements in general can be challenging to compare across the literature due to the different setup conditions[19, 20] and extraction of performance metrics from different curve regimes.[34, 35] The maximum FET hole mobility of 0.56 cm$^2$/Vs was obtained at the critical chain overlap concentration, C*, of 5 g/L and the polymer chain overlap in the solution state appears to contribute to improved charge transport in the solid state. This behavior may be analogous to the tie molecules in high molecular weight P3HT that connect crystalline domains together and improve charge transport.[6, 36-38] A similar trend was observed for hole mobilities extracted from the forward sweep as shown in Figure S12 in the SI. Additionally, for concentrations greater than 5 g/L, we observe greater variations in the hole

mobilities across different OFET devices as represented by the larger error bars. At these concentrations, it is possible that excessive chain entanglement in the solid state leads to spatial defects or charge traps in the thin films. Also, the high viscosity may negatively impact process control during film fabrication, leading to less uniformity. Note that the average threshold voltage increases from 5V to 18V while $I_{on}/I_{off}$ decreases by a factor of 10 with increasing solution concentration, indicating a possible higher density of charge traps. To confirm if this new insight on the key role of solution concentration is potentially general, the previously curated P3HT dataset[19, 20] was revisited to investigate if the data curation approach yields a similar dependance of mobility on concentration. Unlike the DPP-DTT dataset, the algorithm provided a wider range of concentrations to investigate for the P3HT dataset as shown in Figure S15. Concentrations of 5 and 10 g/L suggested by the algorithm do fall in critical chain overlap concentration ranges determined by previous work.[36, 39] It is important to note that the P3HT dataset contains a broader range of $M_w$'s and solvents compared to the DPP-DTT dataset, both of which have been shown to shift the critical overlap concentration.[36] To the best of our knowledge, the influence of solution concentration on FET hole mobility has not been investigated for semicrystalline homopolymers like P3HT, making it difficult to confirm the chain overlap hypothesis suggested by the DPP-DTT exercise. This finding further highlights the need to perform more experiments, not only for D-A polymers like DPP-DTT, but also with semicrystalline homopolymers to investigate the influence of solution concentration on device performance and further strengthen our findings.

In conclusion, we demonstrated that by integrating a data science approach into the existing polymer electronics paradigm, we can gain new insights and guide future experiments to accelerate learning and optimization. The customized classification algorithm when applied to the curated dataset revealed that the polymer solution concentration is an impactful feature that is able to confine "high" performing OFET devices to a reduced design region. Based on the design guidelines suggested by the classification approach, experiments were performed to investigate the influence of solution concentration on the optoelectronic properties of DPP-DTT and confirmed the insights from the data curation exercise. Viscosity measurements of the solutions at different concentrations identified the critical polymer chain overlap concentration occurs at ~ 5 g/L; a result that can be interrogated through future small angle neutron scattering experiments.[23, 39] Application of the weakly-coupled H-J aggregate model to the linear UV-vis absorption spectra revealed that polymer films deposited from semi dilute solutions exhibited a stronger H-type interaction as compared to films prepared from dilute solutions. To gain further insights on the influence of the solution concentration induced chain entanglement on the absorption line shape, transient absorption measurements will be performed to investigate the energetic landscape. Lastly, the electronic performance of the semiconducting thin films prepared from different concentrations was characterized using OFETs. The experimental device results were in good agreement with the design range suggested by the classification algorithm. An increase in the FET hole mobility was observed as the polymer solution concentration approached C*, suggesting that the effective chain overlap is a critical design parameter that impacts charge carrier transport in D-A semiconducting polymers. Our findings highlight the importance of polymer solution concentration as a parameter that must be optimized for the fabrication of conjugated polymer based devices and the critical need to further investigate the impact of this processing parameter to gain a thorough understanding of the process-structure-property relationship.

**Experimental Methods:**

**Database Curation and Classification Analysis :** Detailed explanation of the data curation process and application of the classification algorithm to the dataset along with a github link for the code and dataset is provided in the SI.

**Sample Preparation.** DPP-DTT ($M_w$= 290,000 g $mol^{-1}$, PDI = 2) was purchased from Ossila Limited. For sample preparation, a stock solution of 10 g/L DPP-DTT in chlorobenzene (anhydrous, Sigma-Aldrich) was prepared by heating at 100 ˚C for around 4 hours, followed by heating at 56 ˚C overnight. Solutions with lower concentrations were prepared by diluting the stock solutions. The DPP- DTT thin films are prepared by wire-bar coating the solutions of different concentrations on fused-silica substrates at 56 ˚C followed by annealing for 10 min. A shearing speed of 80 mm/s was used to deposit the films.

**Viscosity Measurement.** The viscosity of the DPP-DTT-Chlorobenzene solutions was measured using a microVISC viscometer (RheoSense, Inc). The solutions can be heated up to 56 ◦C.

**Steady-State Linear Absorption Spectroscopy.** The steady-state linear absorption measurements were performed using a Cary 5000 UV-Vis-NIR spectrometer on the films deposited on glass substrates.

**OFET Fabrication and Characterization.** A detailed explanation of the OFET fabrication and characterization process is provided in the SI and for the most part was consistent with existing literature procedures.

## ASSOCIATED CONTENT

### Supporting Information

The supporting information is available free of charge at:

Dataset and customized classification algorithm details; OFET fabrication and characterization method; Franck Condon fit; AFM and CPOM images; Profilometry results; OFET output and transfer characteristics with explanation for deviation from ideal behavior; DPPDTT solution state UV-Vis spectra.

## AUTHOR INFORMATION

### Corresponding Authors

Martha A. Grover – School of Chemical & Biomolecular Engineering, Georgia Institute of Technology, 311 Ferst Drive, Atlanta, GA, 30332. Email: martha.grover@chbe.gatech.edu

Elsa Reichmanis – Department of Chemical & Biomolecular Engineering, Lehigh University, 111 Research Drive, Bethlehem, PA 18015. Email: elr420@lehigh.edu

**Other Authors**
Aaron Liu - School of Chemical & Biomolecular Engineering, Georgia Institute of Technology, 311 Ferst Drive, Atlanta, GA, 30332;

Carlos Silva - School of Chemistry and Biochemistry, Georgia Institute of Technology, 908 Atlantic Drive, Atlanta, GA, 30332; School of Physics, Georgia Institute of Technology, Atlanta, GA 30332

Campbell Vierson - School of Chemistry and Biochemistry, Georgia Institute of Technology, 801 Atlantic Drive, Atlanta, GA, 30332

Rahul Venkatesh – School of Chemical & Biomolecular Engineering, Georgia Institute of Technology, 311 Ferst Drive, Atlanta, GA, 30332

Yulong Zheng – School of Chemistry and Biochemistry, Georgia Institute of Technology, 801 Atlantic Drive, Atlanta, GA, 30332

**ORCID:**
Elsa Reichmanis: 0000-0002-8205-8016
Martha Grover: 0000-0002-7036-776X
Carlos Silva: 0000-0002-3969-5271
Rahul Venkatesh: 0000-0003-1008-6568
Yulong Zheng: 0000-0001-5136-1971
Aaron Liu 0000-0001-7347-5347

**Notes**
The authors declare no conflict of interest.

**Acknowledgements**
The authors would like to acknowledge the National Science Foundation Grant No. 1922111, DMREF: Collaborative Research: Achieving Multicomponent Active Materials through Synergistic Combinatorial, Informatics-enabled Materials Discovery for support. This work was performed in part at the Georgia Tech Institute for Electronics and Nanotechnology, a member of the National Nanotechnology Coordinated Infrastructure, which is supported by the National Science Foundation (ECCS-1542174); E.R. appreciates support associated with Carl Robert Anderson Chair funds at Lehigh University.

**References**


1. Facchetti, A. π-Conjugated Polymers for Organic Electronics and Photovoltaic Cell Applications. *Chemistry of Materials.* **2011,** *23*, 733-758.

2. Kim, N.-K.; Jang, S.-Y.; Pace, G.; Caironi, M.; Park, W.-T.; Khim, D.; Kim, J.; Kim, D.-Y.; Noh, Y.-Y. High-Performance Organic Field-Effect Transistors with Directionally Aligned Conjugated Polymer Film Deposited from Pre-Aggregated Solution. *Chemistry of Materials.* **2015,** *27*, 8345-8353.

3. Sekine, C.; Tsubata, Y.; Yamada, T.; Kitano, M.; Doi, S. Recent Progress of High Performance Polymer OLED and OPV Materials for Organic Printed Electronics. *Science and Technology of Advanced Materials.* **2014,** *15*, 34203-34218.

4. Zhu, C.; Liu, L.; Yang, Q.; Lv, F.; Wang, S. Water-Soluble Conjugated Polymers for Imaging, Diagnosis, and Therapy. *Chemical Reviews.* **2012,** *112*, 4687-4735.

5. Wunderlich, B. Crystal Structure, Morphology and Defects. In *Macromolecular Physics*, Wunderlich, B., Ed. Academic Press, New York: 1973; Vol. Vol.1

6. Noriega, R.; Rivnay, J.; Vandewal, K.; Koch, F. P. V.; Stingelin, N.; Smith, P.; Toney, M. F.; Salleo, A. A General Relationship Between Disorder, Aggregation and Charge Transport in Conjugated Polymers. *Nature Materials.* **2013,** *12*, 1038-1044.

7. Bao, Z.; Dodabalapur, A.; Lovinger, A. J., Soluble and Processable Regioregular Poly(3-hexylthiophene) for Thin Film Field-Effect Transistor Applications with High Mobility. *Applied Physics Letters.* **1996,** *69*, 4108-4110.

8. Ong, B. S.; Wu, Y.; Liu, P.; Gardner, S. High-Performance Semiconducting

Polythiophenes for Organic Thin-Film Transistors. *Journal of the American Chemical Society.* **2004,** *126*, 3378-3379.

9. Sirringhaus, H.; Brown, P. J.; Friend, R. H.; Nielsen, M. M.; Bechgaard, K.; Langeveld-Voss, B. M. W.; Spiering, A. J. H.; Janssen, R. A. J.; Meijer, E. W.; Herwig, P.; de Leeuw, D. M. Two-Dimensional Charge Transport in Self-Organized, High-Mobility Conjugated Polymers. *Nature.* **1999,** *401*, 685-688.

10. Chang, M.; Choi, D.; Wang, G.; Kleinhenz, N.; Persson, N.; Park, B.; Reichmanis, E. Photoinduced Anisotropic Assembly of Conjugated Polymers in Insulating Polymer Blends. *ACS Appl Mater Interfaces.* **2015,** *7*, 14095-14103.

11. Chen, M.; Peng, B.; Huang, S.; Chan, P. K. L. Understanding the Meniscus-Guided Coating Parameters in Organic Field-Effect-Transistor Fabrications. *Advanced Functional Materials.* **2020,** *30*, 1905963-1905971.

12. Gu, X.; Shaw, L.; Gu, K.; Toney, M. F.; Bao, Z. The Meniscus-Guided Deposition of Semiconducting Polymers. *Nature Communications.* **2018,** *9*, 534-550.

13. Kang, I.; An, T. K.; Hong, J.-a.; Yun, H.-J.; Kim, R.; Chung, D. S.; Park, C. E.; Kim, Y.-H.; Kwon, S.-K. Effect of Selenophene in a DPP Copolymer Incorporating a Vinyl Group for High-Performance Organic Field-Effect Transistors. *Advanced Materials.* **2013,** *25*, 524-528.

14. Lei, Y.; Deng, P.; Li, J.; Lin, M.; Zhu, F.; Ng, T.-W.; Lee, C.-S.; Ong, B. S. Solution-Processed Donor-Acceptor Polymer Nanowire Network Semiconductors For High-Performance Field-Effect Transistors. *Scientific Reports,* **2016,** *6*, 24476-24485.

15. Li, J.; Zhao, Y.; Tan, H. S.; Guo, Y.; Di, C.-A.; Yu, G.; Liu, Y.; Lin, M.; Lim, S. H.; Zhou, Y.; Su, H.; Ong, B. S. A Stable Solution-Processed Polymer Semiconductor with Record High-Mobility for Printed Transistors. *Scientific Reports.* **2012,** *2*, 754-763.

16. Sarkar, T.; Schneider, S. A.; Ankonina, G.; Hendsbee, A. D.; Li, Y.; Toney, M. F.; Frey, G. L. Tuning Intra and Intermolecular Interactions for Balanced Hole and Electron Transport in Semiconducting Polymers. *Chemistry of Materials.* **2020,** *32*, 7338-7346.

17. McBride, M.; Liu, A.; Reichmanis, E.; Grover, M. A. Toward Data-Enabled Process Optimization of Deformable Electronic Polymer-Based Devices. *Current Opinion in Chemical Engineering.* **2020,** *27*, 72-80.

18. Holliday, S.; Donaghey, J. E.; McCulloch, I. Advances in Charge Carrier Mobilities of Semiconducting Polymers Used in Organic Transistors. *Chemistry of Materials.* **2014,** *26*, 647-663.

19. Persson, N.; McBride, M.; Grover, M.; Reichmanis, E. Silicon Valley Meets the Ivory Tower: Searchable Data Repositories for Experimental Nanomaterials Research. *Current Opinion in Solid State and Materials Science.* **2016,** *20*, 338-343.

20. McBride, M.; Persson, N.; Reichmanis, E.; Grover, M. A. Solving Materials'Small Data Problem with Dynamic Experimental Databases. *Processes.* **2018,** *6*, 79-96.

21. Kim, M.; Ryu, S. U.; Park, S. A.; Choi, K.; Kim, T.; Chung, D.; Park, T. Donor–Acceptor-Conjugated Polymer for High-Performance Organic Field-Effect Transistors: A Progress Report. *Advanced Functional Materials.* **2020,** *30*, 1904545-1904570.

22. Liu, A. L.; Venkatesh, R.; McBride, M.; Reichmanis, E.; Meredith, J. C.; Grover, M. A. Small Data Machine Learning: Classification and Prediction of Poly(ethylene terephthalate) Stabilizers Using Molecular Descriptors. *ACS Applied Polymer Materials.* **2020,** *2*, 5592-5601.

23. Zheng, Y.-Q.; Yao, Z.-F.; Lei, T.; Dou, J.-H.; Yang, C.-Y.; Zou, L.; Meng, X.; Ma, W.; Wang, J.-Y.; Pei, J. Unraveling the Solution-State Supramolecular Structures of Donor–Acceptor Polymers and their Influence on Solid-State Morphology and Charge-Transport

Properties. *Advanced Materials.* **2017,** *29*, 1701072-1701080.

24. Porter, R. S.; Johnson, J. F. The Entanglement Concept in Polymer Systems. *Chemical Reviews.* **1966,** *66*, 1-27.

25. Lopes, L. F.; Silveira, B. M.; Moreno, R. Rheological Evaluation of HPAM fluids for EOR Applications. *International Journal of Engineering & Technology.* **2014,** *14*, 35-41.

26. Wood, S.; Wade, J.; Shahid, M.; Collado-Fregoso, E.; Bradley, D. D. C.; Durrant, J. R.; Heeney, M.; Kim, J.-S. Natures of Optical Absorption Transitions and Excitation Energy Dependent Photostability of Diketopyrrolopyrrole (DPP)-Based Photovoltaic Copolymers. *Energy & Environmental Science.* **2015,** *8*, 3222-3232.

27. Qarai, M. B.; Chang, X.; Spano, F. C. Vibronic Exciton Model for Low Bandgap Donor–Acceptor Polymers. *The Journal of Chemical Physics.* **2020,** *153*, 244901-244917.

28. Clark, J.; Chang, J.-F.; Spano, F. C.; Friend, R. H.; Silva, C. Determining Exciton Bandwidth and Film Microstructure in Polythiophene Films using Linear Absorption Spectroscopy. *Applied Physics Letters.* **2009,** *94*, 163306-163311.

29. Hestand, N. J.; Spano, F. C. Expanded Theory of H- and J-Molecular Aggregates: The Effects of Vibronic Coupling and Intermolecular Charge Transfer. *Chemical Reviews.* **2018,** *118*, 7069-7163.

30. Spano, F. C.; Silva, C. H- and J-Aggregate Behavior in Polymeric Semiconductors. *Annual Review of Physical Chemistry.* **2014,** *65*, 477-500.

31. Spano, F. C. Absorption in Regio-Regular Poly(3-hexyl)thiophene Thin Films: Fermi Resonances, Interband Coupling and Disorder. *Chemical Physics.* **2006,** *325*, 22-35.

32. McRae, E. G.; Kasha, M. Enhancement of Phosphorescence Ability upon Aggregation of Dye Molecules. *The Journal of Chemical Physics.* **1958,** *28*, 721-722.

33. Paquin, F.; Yamagata, H.; Hestand, N. J.; Sakowicz, M.; Bérubé, N.; Côté, M.; Reynolds, L. X.; Haque, S. A.; Stingelin, N.; Spano, F. C.; Silva, C. Two-Dimensional Spatial Coherence of Excitons in Semicrystalline Polymeric Semiconductors: Effect of Molecular Weight. *Physical Review B.* **2013,** *88*, 155202-1:14.

34. McCulloch, I.; Salleo, A.; Chabinyc, M. Avoid The Kinks when Measuring Mobility. *Science.* **2016,** *352*, 1521.

35. Sirringhaus, H. 25th Anniversary Article: Organic Field-Effect Transistors: The Path Beyond Amorphous Silicon. *Advanced Materials.* **2014,** *26*, 1319-1335.

36. Hu, H.; Zhao, K.; Fernandes, N.; Boufflet, P.; Bannock, J. H.; Yu, L.; de Mello, J. C.; Stingelin, N.; Heeney, M.; Giannelis, E. P.; Amassian, A. Entanglements in Marginal Solutions: a Means of Tuning Pre-Aggregation of Conjugated Polymers with Positive Implications for Charge Transport. *Journal of Materials Chemistry C.* **2015,** *3*, 7394-7404.

37. Koch, F. P. V.; Rivnay, J.; Foster, S.; Müller, C.; Downing, J. M.; Buchaca-Domingo, E.; Westacott, P.; Yu, L.; Yuan, M.; Baklar, M.; Fei, Z.; Luscombe, C.; McLachlan, M. A.; Heeney, M.; Rumbles, G.; Silva, C.; Salleo, A.; Nelson, J.; Smith, P.; Stingelin, N. The Impact of Molecular Weight on Microstructure and Charge Transport in Semicrystalline Polymer Semiconductors–Poly(3-hexylthiophene), a Model Study. *Progress in Polymer Science.* **2013,** *38*, 1978-1989.

38. Zhao, K.; Khan, H. U.; Li, R.; Su, Y.; Amassian, A. Entanglement of Conjugated Polymer Chains Influences Molecular Self-Assembly and Carrier Transport. *Advanced Functional Materials.* **2013,** *23*, 6024-6035.

39. Lei, S.; Jingnan, Z.; Weiheng, H.; Wenhua, Z.; Liangbin, L. The Effect of Solution Solubility on the Order-Disorder Transition of Molecular Chains in Conjugated Polymer

Solutions. *Acta Polymerica Sinica.* **2019,** *50*, 834-840, DOI: 10.11777/j.issn1000-3304.2019.19023

## TOC Graphic

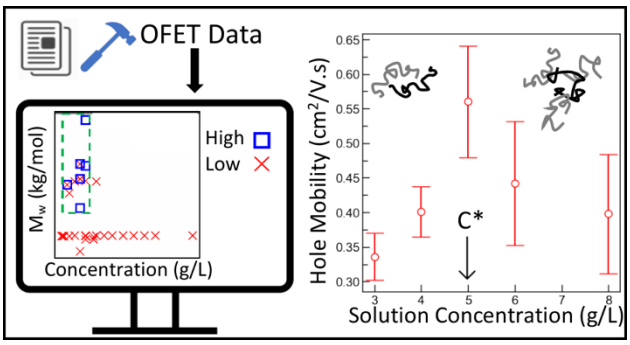
OFET Data
High
Low
$M_w$ (kg/mol)
Concentration (g/L)
Hole Mobility ($cm^2$/V.s)
0.65
0.60
0.55
0.50
0.45
0.40
0.35
0.30
C*
3
4
5
6
7
8
Solution Concentration (g/L)